

INTERNAL BOUNDARY LAYER AFFECTS ON MORPHOLOGIC AND SEDIMENT FLUX TRANSITIONS IN MARS' DUNEFIELDS. K. D. Runyon¹, N. T. Bridges², F. Ayoub³, ¹Johns Hopkins University Department of Earth and Planetary Sciences, Baltimore, MD, USA (kirby.runyon@jhuapl.edu), ²Applied Physics Laboratory, Laurel, MD, USA, ³Caltech, Pasadena, CA, USA,

Introduction and Motivation: Wind mobilizes sediment in four principle ways, each which contributes to the total aeolian sediment flux: saltation, reptation, creep, and suspension [e.g. 1,2]. Saltation (aerodynamic and ballistic grain hop) drives bulk dune formation and movement; reptation (grain splash from saltation) drives ripple formation and movement [3]. Measuring ripple migration on dunes and sand sheets, and dune slip face advancement throughout a dune field, provides a means to quantify the partitioning of sand flux into its constituent processes of saltation and reptation [4,5]. Because dunes and ripple changes can be measured in HiRISE images (down to pixel scales of 25 cm), these processes can be quantified on Mars [4,5,6,7,8].

Studying White Sands, NM, [9] showed an internal boundary layer (IBL) forming over land due to changing surface roughness could accurately predict the observed decrease in sediment flux downwind. Boundary layers thicken down range as momentum changes viscously diffuse through the fluid away from a flow-retarding boundary. Here, we apply [9] & [10]'s IBL approach to Mars to characterize the sediment flux, focusing on Herschel Crater as a case study.

Herschel Crater (14.4°S, 130°E)—a degraded Noachian peak-ring basin almost 300 km in diameter located in the southern highlands—is our study site, as it features multiple aeolian landforms that exhibit clear morphologic transitions (Fig. 1): barchan, barchanoid, and dome dune fields; numerous sand sheets; sand ripples; and indurated transverse aeolian ridges (TARs). It thus serves as a natural laboratory for studying dune and ripple migration rates, sand transport pathways & flux, deposition, erosion rates, sediment sources and sinks, and bedform induration. Here we demonstrate that flux variations within Herschel, and by extension elsewhere on Mars, are due to the formation of an atmospheric IBL created by changing surface roughness. We suggest the bulk dune field remains fixed in location even as individual dunes form, migrate, and disperse.

Methods: HiRISE thrice imaged (PSP_002860_1650 on Mar. 7, 2007; PSP_003572_1650 on May 1, 2007; and ESP_020384_1650 on Dec. 1, 2010) a portion of the dune field in western Herschel Crater. Stereo HiRISE imagery allowed for the production of a DEM [11,12], orthoimagery, and automated ripple change detection [13] between the first and third images. We used ripple displacement and an estimate of height to derive sand

flux from reptation. To measure dune lee front advance rate, we mapped slip face position changes in the latter two images that were co-registered to the first [4,13]. Multiplying this rate by the dune height yielded total bulk sand flux = saltation + reptation + creep [4].

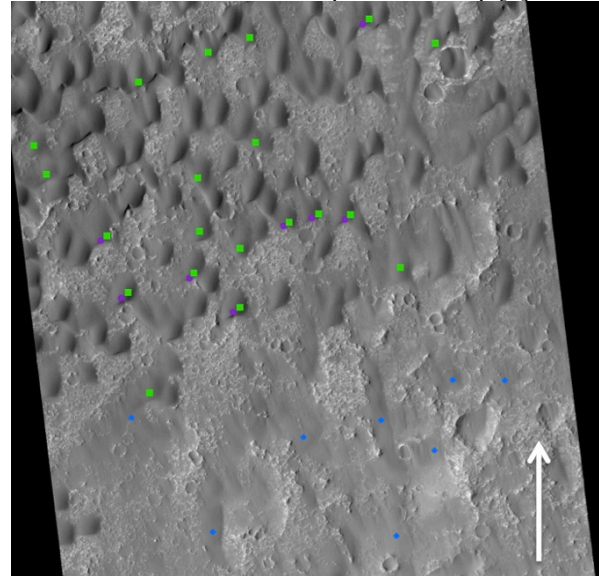


Figure 1. Study area in western Herschel Crater (image PSP_002860_1650). Green squares denote dunes with ripple displacement measurements. Purple dots denote dunes with slip face advancements over 3.74 Earth years. Blue dots denote sand sheets. Arrow points north. The image is approximately 5 km across. Two other overlapping HiRISE images have allowed DEM and ripple displacement map data creation.

To obtain the contribution to total flux from reptation, we used the ENVI module Co-registration of Optically Sensed Images and Correlation (COSI-Corr; [13]) to 1) create orthoimages co-registered to subpixel accuracy; and 2) extract a ripple displacement map by automatically tracking the movement of ripple patterns. Selecting transects along dunes' long axes allowed extraction of both ripple displacement and dune height. We used the same overall procedure as [4].

Results: Presented in Table 1, we report on various bedform metrics. As was found for ripples on dunes in Nili Patera [4], we find a linear relationship between ripple migration rate and their location up the stoss slope of dunes (Figure 2, left). A regression analysis shows there is no significant correlation between the ripple rate slopes (ripple acceleration) and the dune heights, suggesting other factors outweigh ripple acceleration up stoss slopes.

A similar linear trend applies to ripples on extreme downwind undulatory sand sheets (Figure 2, right), though with a notable hysteresis effect: stoss slope

migration rates decrease with downwind distance. This hysteresis may indicate an interplay between the sand sheets' topography and the formation of a secondary IBL: subsequent incipient stoss slopes experience lower ripple rates due to a slowing surface wind [9].

Using a range of estimated and assumed values for wind conditions (5-12 cm-high surface roughness; 0.02-0.04 N/m² wind surface shear stress; 0.02 kg/m³ air density; 2000 m-thick atmospheric boundary layer) [4,10,15] we calculated a range of estimated flux profiles through the dune field as caused by the creation of a hypothetical IBL (Figure 3). The theoretical flux profiles approximately match the observed lee-derived (total) fluxes at the upwind and downwind reaches, though appear inconsistent with midfield observations.

Table 1. Various dune mobility metrics and their values. Years are Earth years. *Estimated value assuming the same flux partition as the downwind dunes.

Metric	Value for Upwind Midfield Downwind Sand Sheet	± 1 σ	Units
Wind Azimuth: speeds > fluid threshold	330	6	Degrees
Advance Rate: Lee (Bulk Dune)	U: 0.271 M: 0.258 D: 0.124 S: -	0.062 0.062 0.038 -	m/yr
Dune Migration Rate: from Reptation	U: - M: - D: 0.032 S: 0.112	- - 0.009 0.077	m/yr
Sand Flux : Reptation	U: - M: - D: 0.316 S: 0.255	- - 0.047 0.073	m ³ /m/yr
Sand Flux : Lee-Based (Total)	U: 4.378 M: 4.559 D: 1.412 S: 1.14*	1.062 1.741 0.315 0.75*	m ³ /m/yr
Height: Mean Dune or Sand sheet	U: 16.917 M: 17.366 D: 10.325 S: 3.057	5.084 3.294 2.821 1.852	m

Table 2. Flux partition results and comparison amongst western Herschel bedforms. Years are Earth years.

Dune Speed	Upwind = 2.2*Downwind
Volumetric Flux	Upwind = 3.1*Downwind
Downwind Dune Flux Partition	Saltation Flux = 3.5*Reptation Flux Total Flux= 4.5*Reptation Flux
Downwind Sand Sheet	Sand sheet reptation flux = 0.81*Downwind Dune reptation flux

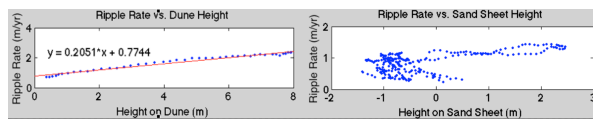


Figure 2. Examples of ripple rates (m/yr) vs. bedform height for downwind dunes (left) and downwind sand sheets (right). They are generally positively correlated as was seen by [4] for Nili Patera ripples. The undulatory topography of the sand sheets leads to hysteresis in the ripple rate.

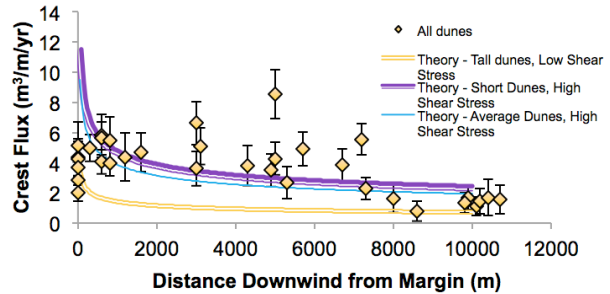


Figure 3. Predicted declining flux curves from the thickening IBL envelop the range of wind and surface variables expected for the western Herschel. The predictions match observed upwind and downwind fluxes, and the anomalously high medial fluxes are likely from a local ridge. Small sand sheets at the most distal portions have estimated total fluxes from assuming the same reptation-flux:total-flux partition as the downwind dome and barchan dunes.

Discussion and Conclusion: Sand flux is partitioned such that saltation is 3.5x the reptation flux (Table 2), which is very close to the value of 4 measured by [4] for Nili Patera dune field's upwind barchan dunes. The bedforms' average total flux of 3.4 m³/m/yr is roughly half of Nili Patera's 6.9 m³/m/yr; this should not be surprising because Nili dunes are nearly twice as tall (22 ± 9 m, [4]) as Herschel dunes (14 ± 5 m).

Herschel's peak-ring seems to control the upwind boundary location of the dune field, likely through its creation of an IBL. Additionally, a topographic ridge in the upwind/midfield region of the dune field likely accelerates the wind from streamline compression, allowing the dune height and flux to actually increase (Figure 3) for a certain distance downwind before the dune-enhanced IBL begins to dominate again, serving to decrease the flux and dune height. This interplay in wind obstacles and surface roughness may explain the high midfield flux anomalies & the flux profile overall.

IBLs from non-aeolian surface roughness elements in Herschel seem to determine the location of bedforms. Extrapolating across Mars, we predict IBLs from non-aeolian topography will control the locations of other aeolian provinces.

References: [1] Bagnold R. A. (1941) *Dover 0-486-43931-3*. [2] Kok J. F. et al. (2012) *Rep. Prog. Phys.* 75, 106901. [3] Anderson, R.S. (1987) *Sedimentology* v. 34, no. 5, p. 943-956, doi: 10.1111/j.1365-3091.1987.tb00814.x [4] Bridges N. T. et al. (2012) *Nature* 485, 339, doi:10.1038/nature11022. [5] Ayoub, F., et al., (2014), *Nature Communications*, DOI: 10.1038/ncomms6096 [6] Bridges et al., (2012), *Geology*, v. 40, no. 1, p. 31-34. [7] Ewing, R.C., Peyret, A.-R.B., Kocurek, G., Bourke, M., (2010), *JGR-P*, DOI: 10.1029/2009JE003526. [8] Chojnacki, M., Burr, D.M., Moersch, J.E., Michaels, T.I. (2011), *JGR*, doi:10.1029/2010JE003675. [9] Jerolmack, D.J. et al., (2012), *Nature Geoscience*, DOI:10.1038/NGEO1381. [10] Lettau, H. (1969), *J. Appl. Meteorol.* 8, 828-832. [11] Kirk, R. et al. *7th International Conf. Mars*, 3381 Pasadena, CA (2008). [12] Mattson, S. et al., (2009), *European Planetary Science Congress, EPSC2009-604*. [13] Leprince S. et al., (2007) *IEEE Trans. Geosci. and Rem. Sensing*, 45, 6. [14] Bridges et al., (2013) *Aeolian Research*, 9, p. 133-151. [15] Haberle, R.M., Murphy, J.R., Schaeffer, J. (2003), *Icarus*, 161, 66-89.